A Multiscale Approach to Estimate Large Scale Flow and Leakage from Geological Storage

Master of Science Thesis in Applied Mathematics

Elin Marie Elje

Department of Mathematics
University of Bergen
Norway

June 2010

Acknowledgments

I would like to thank my supervisors Jan Martin Nordbotten and Eirik Keilegavlen for their helpfulness and enthusiasm. To all my friends and fellow students at the institute, thank you for five enjoyable years.
Last but not at least, a special thank to my parents for always being there. I did it!

Abstract

Deep saline aquifers offer the greatest storage capacity for geological storage. However, the formations might be extensive and because of the oil and gas legacy the aquifers are frequently perforated by abandoned wells. These wells becomes potential leakage pathways for the injected CO_2. There might be as many as hundreds of thousands abandoned wells in a saline aquifer, which make obtaining accurate and robust estimates for the flow in these systems a major challenge.

In this thesis a multiscale approach have been used to couple a FEM well leakage model and a ELSA well leakage model, in order to achieve a multiscale model that would estimate the large scale flow and leakage from geological storage on extensive domains. In the search after a radius for the fine scale solver it was discovered that a well is hardly affected by the coarse scale solution, due to the radius of influence of a well. Hence, the derived model is not a multiscale model and is not able to estimate the flow in the system.

Contents

Introduction

Geological storage is one strategy for reducing CO_2 emissions to the atmosphere. Suitable geological formations for CO_2 storage are oil and gas reservoirs, deep saline aquifers, coal seams and salt caverns. To each of the potential storage sites, there are advantages and disadvantages. Deep saline aquifers offer the greatest storage capacity, estimated between 300 and 10,000 $GtCO_2$ [1], and one can take advantage of the existing infrastructure and experience associated with the enhanced oil recovery. Saline aquifers are saturated with water that has a high salt concentration. This water is referred to as brine. While seawater has a salinity about 35,000 parts per million, the deep formations may have a salt concentration of several hundreds of thousands parts per million [2]. Because of the oil and gas legacy, aquifers are frequently perforated by abandoned wells. These abandoned wells become potential leakage pathways for the brine and the injected CO_2. As leakage of CO_2 may pollute oil and gas resources or leak to the atmosphere, brine may pollute drinking waters because of its high salt concentration. Therefore, in order to do large scale deployment of CO_2, tools for estimating the flow of CO_2 and brine are essential.

An aquifer may be perforated by hundreds of thousands of abandoned wells, and between the surface and the injection aquifer there are often five to ten aquifers. Large scale deployment of CCS may also necessitate multiple injection sites within the same aquifer. Obtaining accurate and robust estimates for this system is a major challenge. Well leakage models have been developed in order to estimate flow and leakage. However, for extensive domains with the possibility of hundreds of thousands of abandoned wells, the system would be too complicated to solve. Therefore, an idea is to use a well leakage model on a coarse scale and one on a fine scale. By combining these in a multiscale system, one may be able to estimate large scale flow and leakage on extensive domains. The first step in developing such a model is to consider a simplified system with a single-phase flow of water. In chapter 1, an introduction is given

to groundwater flow, where an equation for the groundwater flow is derived followed by a presentation of a real groundwater system. Chapter 2 introduces two solution approaches to the groundwater equation, and chapter 3 uses these approaches in deriving a multiscale model to estimate large scale flow and leakage. However, in the determination of the length of the fine scale domains, it becomes clear that the derived model do not have a multiscale structure. In chapter 4, the behavior of the well leakage models derived in chapter 2 and 3 are illustrated for basic examples. Finally, conclusions are made in chapter 5.

Chapter 1

Groundwater Flow

In this chapter, a foundation for analyzing groundwater flow will be presented. Important definitions regarding flow in aquifers are given, followed by a derivation of a groundwater flow equation. This equation takes into account the possibility of injection, pumping and abandoned wells located in an aquifer. The chapter ends by presenting a real groundwater flow problem.

1.1 Geological formations

Groundwater is a term used for water positioned beneath the ground surface. The ground can be considered as more or less vertically layered. These layers have different properties, where a region consisting of essentially the same properties is called a formation. The vertical layers are porous media, and they are often divided into three categories; aquifers, aquitards and aquicludes. Figure 1.1 illustrates an example of a common composition of these layers.

An aquifer contains water and has a relatively low resistance to flow. This implies that a significant amount of water can be moved through the material. The horizontal dimension of an aquifer may be extensive and is usually between 3 to 50 kilometers. The thickness of an aquifer is significantly less, generally in the range of 5 to 200 meters.

The water table is a surface in the formation indicating where the pressure equals the atmospheric pressure. Depending on the position of the water table, aquifers can be classified as unconfined or confined, see [3] for more details.

An *unconfined aquifer* is capable of receiving water through the upper boundary, and is therefore referred to as a "water-table aquifer" because

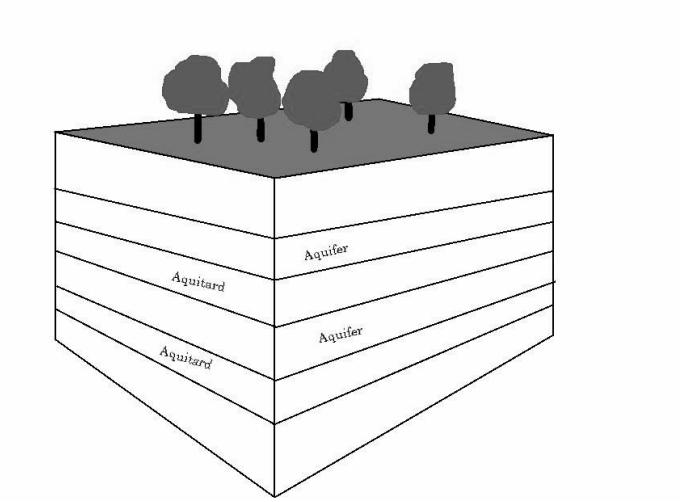

Figure 1.1: A common structure of a geological formation, where aquifers are separated by aquitards.

of the location of the water table in the aquifer. The upper boundary is then a transition zone, and the remaining zone in the layer is filled with fluids.

A *confined aquifer* is an aquifer that is confined between two formations with significantly less ability to flow.

An aquiclude is a formation that may contain fluids, but transmits them in a significant smaller quantity then an aquifer. In the study of groundwater flow an aquiclude is considered impervious.

Aquitards are formations that are capable of transmitting fluids at a very slow rate. However, if an aquitard is situated between two aquifers, it may transmit a large amount of fluids essentially vertically between the aquifers. The aquifer that the aquitard extracts fluids from, is then called a leaky aquifer. For more details see [3].

1.2 Flow in a Porous Medium

A porous medium is a medium consisting of pores. About all materials in the nature can be considered as porous media [4], i.e. they are composed by solids and pores. Hence, in order to estimate groundwater flow, an understanding of the flow through porous media is crucial.

The pores may be isolated or connected. In connected pores, fluids can flow in various rates depending on the properties of the medium and

the fluid. The solid medium is called the solid matrix, and the space within a medium that is not a part of the solid medium is called the void space, also known by the term pore space. The volume of connected pores may be denoted as the effective pore volume, where the unconnected pores can be considered part of the solid matrix. Figure 1.2 illustrates an example of a porous medium.

The microscopic information about the structure of a porous medium is often unknown. The irregularities in a pore structure can be considered as random variations with a well defined average, and quantities such as velocity and pressure may be defined as an average over a reference volume. In literature the reference volume is called a representative elementary volume (REV) [3]. When introducing a reference volume, the properties of a porous medium is characterized by its porosity and permeability. Hence, it is possible to derive a macroscopic model of the flow through a medium.

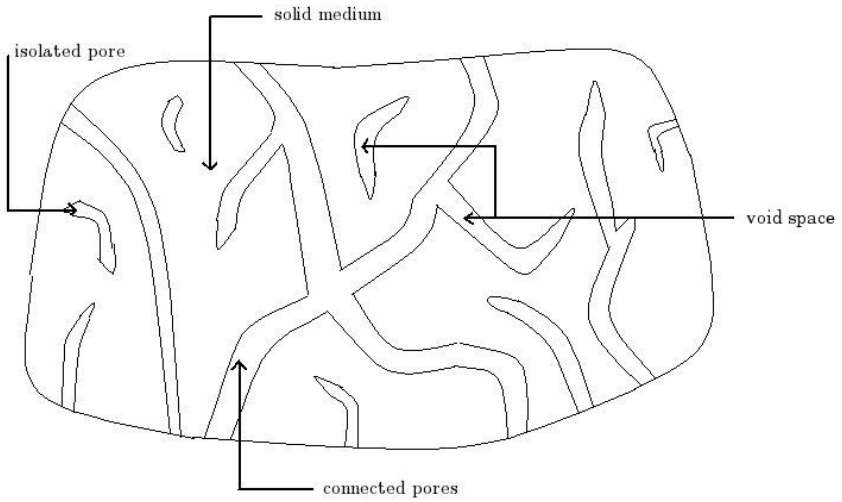

Figure 1.2: An illustration of the structure of a porous medium consisting of the solid matrix and the isolated and connected pores.

1.2.1 Porosity

Porosity is a quantity indicating the amount of effective pore space available to be filled with fluids. The ratio of the effective pore space and the total volume defines the porosity

$$\phi \stackrel{def}{=} \frac{V_{pores}}{V_{tot}}, \tag{1.1}$$

where V_{pores} is the volume of effective pore space and V_{tot} is the total volume of the medium. The volume of the solid medium V_{solids} and the void space V_{voids} forms the total volume, $V_{tot} = V_{solids} + V_{voids}$.

1.2.2 Conservation of Mass

A formulation of mass conservation can be found by considering an arbitrary fixed geometrical volume Ω, see figure 1.3. The change of mass inside Ω is balanced by mass flow into the volume through its boundaries, and by sources and sinks within the volume.

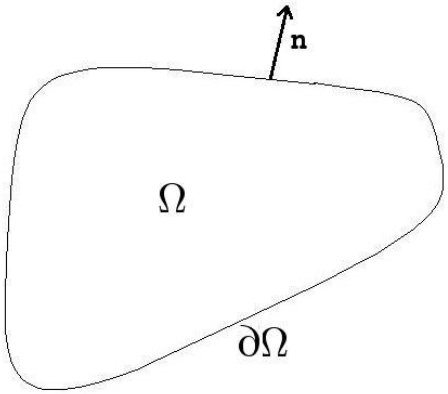

Figure 1.3: An arbitrary fixed geometrical volume Ω, with surface $\partial\Omega$ and outer normal unit vector $\mathbf{n}$.

Fluid density ρ is defined as mass of fluid per unit volume. Hence, the mass of a fluid can be expressed as $\int_\Omega \phi\rho dV$. Inflow and outflow through the boundaries may be formulated as the fluid density multiplied by the flux vector, $\mathbf{u}$, multiplied with a unit vector, $\mathbf{n}$. The unit vector is directed outward and normal to the surface $\partial\Omega$. The volumetric source or sink term is denoted by Q, and sources or sinks of mass within the volume is expressed as ρQ. A mass conservation equation can be formulated as

$$\frac{\partial}{\partial t}\int_\Omega \phi\rho d\tau \; + \; \int_{\partial\Omega} (\rho\mathbf{u})\cdot\mathbf{n} d\sigma \; = \; \int_\Omega \rho Q d\tau. \tag{1.2}$$

Gauss's theorem states the following relationship for sufficiently smooth functions $\int_{\partial\Omega} \rho\mathbf{u}\cdot\ \mathbf{n}d\sigma \; = \; \int_\Omega \nabla\cdot(\rho\mathbf{u})d\tau$. The theorem applied to equation (1.2) gives

$$\frac{\partial}{\partial t}\int_{\Omega}\phi\rho d\tau \; + \; \int_{\Omega}\nabla\cdot(\rho\mathbf{u})d\tau \; = \; \int_{\Omega}\rho Q d\tau. \tag{1.3}$$

Since the volume Ω is a geometrically fixed volume, Ω is not a function of time. The derivative with respect to time in equation (1.3) may then be placed inside the integral, which gives

$$\int_{\Omega}\left[\frac{\partial}{\partial t}(\phi\rho) + \nabla\cdot(\rho\mathbf{u}) - \rho Q\right]d\tau = 0. \tag{1.4}$$

Because the integral in equation (1.4) must hold for any arbitrary closed volume and by assuming continuity of the solution, the mass balance equation can be given on a differential form

$$\frac{\partial(\phi\rho)}{\partial t} + \nabla\cdot(\rho\mathbf{u}) = \rho Q. \tag{1.5}$$

The conservation of mass equation (1.5), will be further used in the derivation of a governing groundwater flow equation in section 1.4.

1.2.3 Hydraulic Head

An important quantity in groundwater hydrology is the hydraulic head. This property is a direct measure of energy or potential of a fluid expressed in length units. For more information see [2]. The hydraulic head is defined as

$$h \overset{def}{=} \frac{p}{\rho g} + z, \tag{1.6}$$

where p is the pressure, g is the gravitational constant and z is the vertical position from the defined origin.

1.2.4 Darcy's Law and Hydraulic Conductivity

Darcy's law is a fundamental law in fluid dynamics. The law presents an expression for the volumetric flux, $\mathbf{u}$; volume of fluid passing through a porous medium per cross sectional area. The law may be stated as

$$\mathbf{u} = -\mathbf{K}\cdot\nabla\mathbf{h}, \tag{1.7}$$

where $\mathbf{K}$ is the hydraulic conductivity and $\mathbf{h}$ is the hydraulic head. The hydraulic conductivity expresses the ability of an aquifer to transport fluids through its material under hydraulic gradients, and is defined as

$$\mathbf{K} \stackrel{def}{=} \frac{\mathbf{k}\rho g}{\mu}, \tag{1.8}$$

where $\mathbf{k}$ is the permeability and μ is the viscosity. The permeability is a measure of the ability of a matrix to transmit fluids through its material. Even though the permeability only depends on the medium, the hydraulic conductivity depends on both the medium and the fluid.

In accordance with Darcy's Law (1.7), a fluid in a porous medium will flow from regions with higher values of hydraulic head to regions with lower values.

1.3 Groundwater Flow Properties

To derive a groundwater flow equation, parameters regarding the medium and the water must be defined. In this section definitions of the compressibility of water and the medium is introduced, followed by an expression for the storativity. These expressions are needed in the derivation of the groundwater flow equation from the mass conservation equation in section 1.4.

1.3.1 Compressibility and Effective Stress

Compressibility is a material property describing change in volume, or strain, due to an applied stress on a material.

Compressibility of Water

The stress of a fluid depends on the fluid pressure. Since the fluid in this context is water, the fluid compressibility equals the ratio between the change in the water volume and the change in pressure [5]. This definition can be formulated as

$$\beta \stackrel{def}{=} -\frac{1}{V_w}\frac{dV_w}{dp}, \tag{1.9}$$

where the compressibility of water is denoted by β and the water volume by V_w. From [3], the compressibility of water can also be formulated as

$$\beta = \frac{1}{\rho}\frac{d\rho}{dp}, \tag{1.10}$$

because the density and the volume are related as $\rho = \frac{m}{V}$.

Effective Stress

The pressure of the water in the pores and the solid matrix forms the total stress σ_{tot}, and is defined as

$$\sigma_{tot} \stackrel{def}{=} \sigma_{eff} + p. \tag{1.11}$$

The effective stress σ_{eff} is the portion of the total stress that is not caused by the fluid. The weight of rock and water overlying each point in the system, can be considered constant through time. This implies $\frac{\partial \sigma_{tot}}{\partial t} = 0$, and the change in effective stress with respect to time equals the negative change of pressure,

$$\frac{\partial \sigma_{eff}}{\partial t} = -\frac{\partial p}{\partial t}. \tag{1.12}$$

From the definition of hydraulic head in equation (1.6), the pressure can be expressed as $p = \rho g(h - z)$. The change in pressure is then $\frac{\partial p}{\partial t} = \rho g \frac{\partial h}{\partial t}$. Inserted in equation (1.12), the expression for the change in effective stress can be rewritten as

$$\frac{\partial \sigma_{eff}}{\partial t} = -\rho g \frac{\partial h}{\partial t}. \tag{1.13}$$

Compressibility of a Porous Medium

The compressibility of a porous medium, α, equals the ratio between the change in volume of a porous medium and the change in the effective stress,

$$\alpha \stackrel{def}{=} -\frac{1}{V_{tot}} \frac{dV_{tot}}{d\sigma_{eff}}. \tag{1.14}$$

The total volume of a porous medium is defined in section 1.2.1 as $V_{tot} = V_{solids} + V_{voids}$. Since the soil grains usually do not deform but may reorient themselves, the change in the total volume is approximate the change in pore volume, $\frac{\partial V_{tot}}{\partial t} \approx \frac{\partial V_{voids}}{\partial t}$. By equation (1.1) and equation (1.12) the compressibility of the porous medium becomes

$$\alpha \approx \frac{d\phi}{dp}. \tag{1.15}$$

1.3.2 Storativity

Specific Storativity

The specific storativity S_s of a saturated aquifer is defined as the volume of water a unit volume of an aquifer releases from storage under a unit decline in hydraulic head [5]. Water is released from storage by the compaction of an aquifer and by water expansion. Due to compaction, $\frac{\partial V_{tot}}{\partial t}$ will be negative. However, the expelled water $\frac{\partial V_{Wc}}{\partial t}$ will be positive. Hence, $\frac{\partial V_{Wc}}{\partial t} = -\frac{\partial V_{tot}}{\partial t}$. From equation (1.14), the produced water can then be expressed as

$$\frac{\partial V_{Wc}}{\partial t} = \alpha V_{tot} \frac{\partial \sigma_{eff}}{\partial t}. \tag{1.16}$$

For a unit total volume, $V_{tot} = 1$. Equation (1.13) inserted in equation (1.16) with the unit decline in hydraulic head, $\frac{\partial h}{\partial t} = -1$, gives that the water produced by the compaction of the aquifer can be stated as

$$\frac{\partial V_{Wc}}{\partial t} = \alpha \rho g. \tag{1.17}$$

The volume of water produced by an expansion of water, $\frac{\partial V_{We}}{\partial t}$, can be obtained from equation (1.9), where in the total unit volume there is a water volume of $V_W = \phi V_{tot}$, and the change in pressure can be expressed as $\frac{\partial p}{\partial t} = -\rho g$. The volume of water produced by water expansion is then

$$\frac{\partial V_{We}}{\partial t} = \beta \phi \rho g. \tag{1.18}$$

A summation of the water produced by a compaction of the aquifer and an expansion of the water defines the specific storage,

$$S_s = \frac{\partial V_{Wc}}{\partial t} + \frac{\partial V_{We}}{\partial t} = \rho g(\alpha + \phi\beta). \tag{1.19}$$

Storativity

The storativity is a measure of the water volume released from a vertical column of aquifer per unit decline in hydraulic head. For a confined aquifer of thickness D, the storativity is defined as the specific storage times the thickness,

$$S = S_s D = \rho g D(\alpha + \phi\beta). \tag{1.20}$$

1.4 The Groundwater Flow Equation

In this section a groundwater flow equation in terms of the hydraulic head will be derived. The derivation begins by recalling the mass conservation equation (1.5),

$$\frac{\partial(\phi\rho)}{\partial t} + \nabla \cdot (\rho \mathbf{u}) = \rho Q. \tag{1.21}$$

The partial derivative of the porosity and the density in equation (1.21) can be expressed in terms of the derivative of the pressure,

$$\frac{\partial(\phi\rho)}{\partial t} = \phi\frac{\partial\rho}{\partial t} + \rho\frac{\partial\phi}{\partial t} = \phi\frac{d\rho}{dp}\frac{\partial p}{\partial t} + \rho\frac{d\phi}{dp}\frac{\partial p}{\partial t}. \tag{1.22}$$

The definition of the compressibility of water, equation (1.10), implies $\frac{d\rho}{dp} = \beta\rho$. Equation (1.15), and the assumption that the change in total volume only depends on the change in the volume of voids, implies $\frac{d\phi}{dp} = \alpha$. When substituting the derivative terms, equation (1.22) becomes

$$\frac{\partial(\phi\rho)}{\partial t} = \rho(\phi\beta + \alpha)\frac{\partial p}{\partial t}. \tag{1.23}$$

The derivative of the pressure with respect to time is related to change in the hydraulic head, $\frac{\partial p}{\partial t} = \rho g\frac{\partial h}{\partial t}$. By substituting the pressure derivative, equation (1.23) turns into

$$\frac{\partial(\phi\rho)}{\partial t} = \rho^2 g(\phi\beta + \alpha)\frac{\partial h}{\partial t}, \tag{1.24}$$

where the term $\rho g(\phi\beta+\alpha)$ is the specific storativity from equation (1.19). Equation (1.24) then becomes

$$\frac{\partial(\phi\rho)}{\partial t} = \rho S_s\frac{\partial h}{\partial t}. \tag{1.25}$$

The mass conservation equation (1.21) inserted (1.25) returns

$$\rho S_s\frac{\partial h}{\partial t} + \nabla \cdot (\rho \mathbf{u}) = \rho Q. \tag{1.26}$$

1.4.1 Reduction in Dimensionality

When the density is assumed to be constant in space, the conservation equation (1.26) may be expressed as

$$S_s \frac{\partial h}{\partial t} + \nabla \cdot \mathbf{u} = Q. \tag{1.27}$$

Equation (1.27) is a three-dimensional equation. Due to the aquifers extensive horizontal length compared to the vertical length, its of interest to model the problem without taking into account variations in the vertical. The equation will then be a two-dimensional equation, only depending on the horizontal position within the aquifer. In that procedure, equation (1.27) is integrated in the vertical direction. Figure 1.4 is an example of the integral direction. The top and the bottom boundary of the aquifer in the vertical are denoted by $\zeta_T(x_1, x_2)$ and $\zeta_B(x_1, x_2)$, and the integral of equation (1.27) becomes

$$\int_{\zeta_B}^{\zeta_T} S_s \frac{\partial h}{\partial t} dz + \int_{\zeta_B}^{\zeta_T} \nabla \cdot \mathbf{u} dz = \int_{\zeta_B}^{\zeta_T} Q dz. \tag{1.28}$$

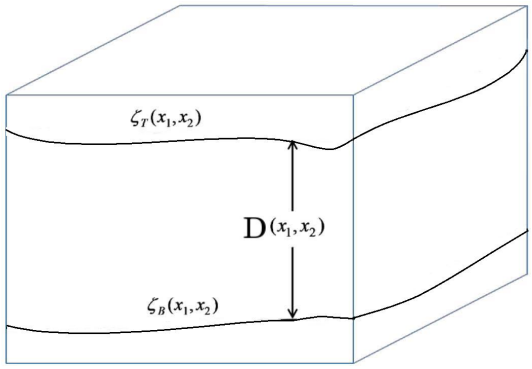

Figure 1.4: An illustration of the vertical boundaries for an aquifer where ζ_T is the upper boundary, ζ_B is the bottom boundary and D is the thickness of the aquifer. Adapted from [2].

The specific storativity is assumed to be constant with respect to variations in the vertical direction. Further, the top and the bottom boundary of the aquifer is assumed to be independent of time, thus

$$\int_{\zeta_B}^{\zeta_T} S_s \frac{\partial h}{\partial t} dz = S_s \frac{\partial}{\partial t} \int_{\zeta_B}^{\zeta_T} h dz = S_s D \frac{\partial \overline{h}}{\partial t}. \tag{1.29}$$

In equation (1.29), D is denoted as the length between the top and bottom boundary and defines the aquifers thickness. The vertical averaged hydraulic head $\overline{h}$ is defined as

$$\overline{h}(x_1, x_2, t) = \frac{1}{D}\int_{\zeta_B}^{\zeta_T} h(x_1, x_2, z, t)dz. \tag{1.30}$$

The divergence of the flux in the second term in equation (1.28), may be written in terms of the three spatial components

$$\int_{\zeta_B}^{\zeta_T} \nabla \cdot \mathbf{u}dz = \int_{\zeta_B}^{\zeta_T} \left(\nabla_{||} \cdot \mathbf{u}_{||} + \frac{\partial}{\partial z}u_z\right)dz, \tag{1.31}$$

where $\nabla_{||} = \frac{\partial}{\partial x_1}\mathbf{e}_1 + \frac{\partial}{\partial x_2}\mathbf{e}_2$. Leibniz's rule applied on the first term in the integral in equation (1.31) gives

$$\int_{\zeta_B}^{\zeta_T} \nabla_{||} \cdot \mathbf{u}_{||}dz = \nabla_{||} \cdot \int_{\zeta_B}^{\zeta_T} \mathbf{u}_{||}dz - \mathbf{u}_T \cdot \nabla\zeta_T + \mathbf{u}_B \cdot \nabla\zeta_B, \tag{1.32}$$

where $\mathbf{u}_T$ and $\mathbf{u}_B$ denotes the flow vector at the top and bottom of the aquifer and $\nabla\zeta_T$ and $\nabla\zeta_B$ are the normal directions to the top and bottom boundary. From the Fundamental Theorem of calculus, the second term in equation (1.31) becomes

$$\int_{\zeta_B}^{\zeta_T} \frac{\partial}{\partial z}u_z dz = \mathbf{u}_T \cdot \mathbf{e}_z - \mathbf{u}_B \cdot \mathbf{e}_Z. \tag{1.33}$$

Equation (1.32) and (1.33) inserted in equation (1.31) returns

$$\int_{\zeta_B}^{\zeta_T} \nabla \cdot \mathbf{u}dz = \nabla_{||} \cdot \int_{\zeta_B}^{\zeta_T} \mathbf{u}_{||}dz + \mathbf{u}_T \cdot (\mathbf{e}_z - \nabla\zeta_T) - \mathbf{u}_B \cdot (\mathbf{e}_Z - \nabla\zeta_B). \tag{1.34}$$

The evaluation at the top and bottom of the formation are for simplicity denoted by $\psi_T = \mathbf{u}_T \cdot (\mathbf{e}_z - \nabla\zeta_T)$ and $\psi_B = \mathbf{u}_B \cdot (\mathbf{e}_Z - \nabla\zeta_B)$. When denoting the flow vector $\mathbf{u}$ in the x_1 and x_2 direction as

$$\mathbf{U}(x_1, x_2, t) = \int_{\zeta_B}^{\zeta_T} \mathbf{u}_{||}dz, \tag{1.35}$$

equation (1.28) can be written as

$$S_s D\frac{\partial \overline{h}}{\partial t} + \nabla_{||} \cdot \mathbf{U} + \psi_T - \psi_B = \int_{\zeta_B}^{\zeta_T} Qdz = \overline{Q}, \tag{1.36}$$

where $\overline{Q}$ represents the vertically integrated source or sink term.

Recall the specific discharge in equation (1.27). From Darcy's Law, equation (1.7), the specific discharge can be formulated as $\nabla \cdot \mathbf{u} = -\nabla \cdot (\mathbf{K} \cdot \nabla \mathbf{h})$ and

$$\mathbf{U}(x_1, x_2, t) = -\int_{\zeta_B}^{\zeta_T} \mathbf{K} \cdot \nabla \mathbf{h} \; dz. \tag{1.37}$$

Because the layered structure in most porous media is roughly horizontal, the direction of the hydraulic conductivity aligns with the vertical and the horizontal directions [2]. The hydraulic conductivity can then be formulated as a block-diagonal matrix,

$$\mathbf{K} = \begin{bmatrix} K_{1,1} & K_{1,2} & 0 \\ K_{2,1} & K_{2,2} & 0 \\ 0 & 0 & K_z \end{bmatrix} = \begin{bmatrix} \mathbf{K}_{||} & \mathbf{0} \\ \mathbf{0} & K_z \end{bmatrix}.$$

An assumption that the horizontal flow directions dominates the system, vertical flows will be insignificant within the formation and the hydraulic head will be essentially constant along the vertical direction. For vertical variations in the head represented by $\widetilde{h} = h - \overline{h}$, equation (1.37) can be approximated [2],

$$\begin{aligned} \mathbf{U} &= -\int_{\zeta_B}^{\zeta_T} \left(\mathbf{K}_{||} \nabla_{||} h + K_z \frac{\partial h}{\partial z} \right) dz \\ &= -D\overline{\mathbf{K}}_{||} \nabla_{||} \overline{h} + \int_{\zeta_B}^{\zeta_T} \left(\mathbf{K}_{||} \nabla_{||} \widetilde{h} + K_z \frac{\partial \widetilde{h}}{\partial z} \right) dz \\ &\approx -D\overline{\mathbf{K}}_{||} \nabla_{||} \overline{h}. \end{aligned} \tag{1.38}$$

In equation (1.38), the vertical averaged hydraulic conductivity is denoted $\overline{\mathbf{K}}$. The flow in the aquifer is assumed essentially horizontal, which implies that $D\overline{\mathbf{K}}_{||}$ expresses the aquifers ability to transmit water through its entire thickness. This description of the aquifer is called the transmissivity $\mathbf{T}$, and is defined as

$$\mathbf{T}(x_1, x_2) = \int_{\zeta_B}^{\zeta_T} \mathbf{K}(x_1, x_2, z) dz = \overline{\mathbf{K}}(x_1, x_2) D(x_1, x_2). \tag{1.39}$$

Equation (1.39) and the definition of storativity, equation (1.20), inserted in equation (1.36) returns

$$S \frac{\partial \overline{h}}{\partial t} - \nabla_{||} \cdot (\mathbf{T} \cdot \nabla_{||} \overline{h}) + \psi_T - \psi_B = \overline{Q}. \tag{1.40}$$

Equation (1.40) is a two dimensional single phase flow equation in terms of the hydraulic head.

1.4.2 Simplifying Assumptions

Simplifications to equation (1.40) can be made. In this context the formation is assumed to be *isotropic*, which implies that the transmissivity matrix is a diagonal matrix where both entries are the same. A scalar can then replace the transmissivity matrix. The formation is also assumed to be *homogeneous*, resulting in the transmissivity to be independent of space. These simplifications applied on equation (1.40) gives the governing groundwater flow equation,

$$S\frac{\partial \overline{h}}{\partial t} - T\nabla^2\overline{h} + \psi_T - \psi_B = \overline{Q}. \tag{1.41}$$

In the following chapters the vertical averaged terms in equation (1.41) will not be denoted by an overline.

1.5 A Real Groundwater System

An example of a real groundwater system is the Alberta Basin located in western Canada, see figure 1.5. Because of its large oil and gas fields, it is a major North American energy producer. The oil and gas exploration began in the late 19th century, and a major oil discovery in 1947 resulted in a rapid growth that even continues today. New wells are being drilled at a rate of approximately 12 000/yr and in 2003 more than 320 000 wells had been drilled [1]. These wells are distributed over most of the basin area, which covers more than 900 000 km^2. The formation is deepest along its western boundary, where it is more than 3000 m deep, and slopes upward toward the northeast.

The Viking Formation, which has an areal extent that covers much of the basin, contains approximately 5% of the oil reserves and 8% of the gas reserves in the Alberta Basin. The cross section of the Alberta Basin in figure 1.5 illustrates the location of the Viking aquifer. Several studies on the suitability and capacity for CO_2 sequestration have focused on the Viking aquifer. The Viking Formation consists mostly of sandstone that are saturated with saline water, forming an aquifer. The aquifer covers an area of 468 000 km^2 and the thickness of the aquifer varies from a few meters to more than 120 m. Bachu and Adams have shown that significant parts of the Viking aquifer are suitable for CO_2 sequestration based on depth and capacity considerations and the presence of a thick caprock overlying the entire formation [1]. The ultimate capacity of the Viking aquifer based on the amount of CO_2, was estimated to be in the

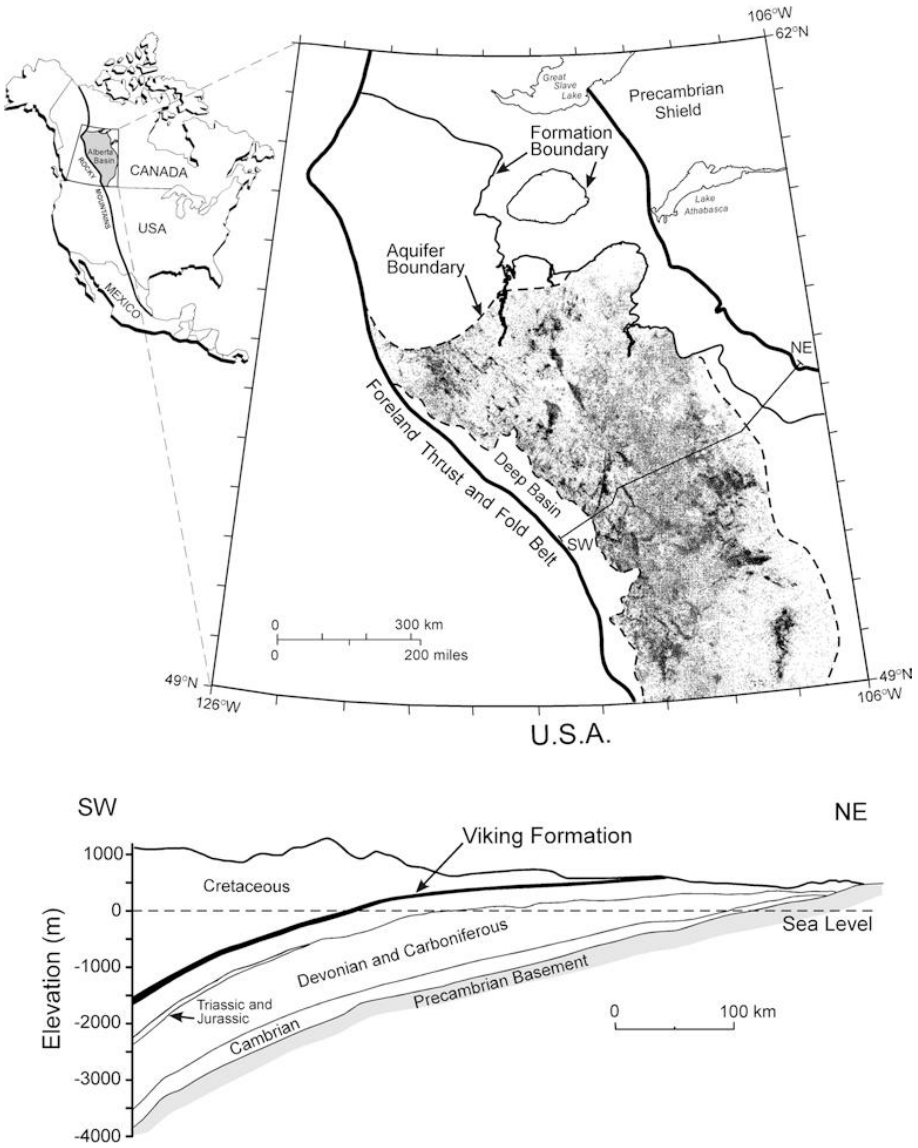

Figure 1.5: The Alberta Basin and the Viking aquifer in Canada. Adapted from [1].

order of 100 $GtCO_2$. However, more than 200 000 wells have been drilled through the Viking Formation. The wells are distributed over most of the 468 000 km^2 area and over half of all wells that penetrate the Viking aquifer are classified as abandoned wells. Some of the wells that penetrate it produces from the Viking formation while others pass through on their way to deeper producing formations. In figure 1.6 the extensiveness of

the flow problem is illustrated by the location of all the wells in Alberta.

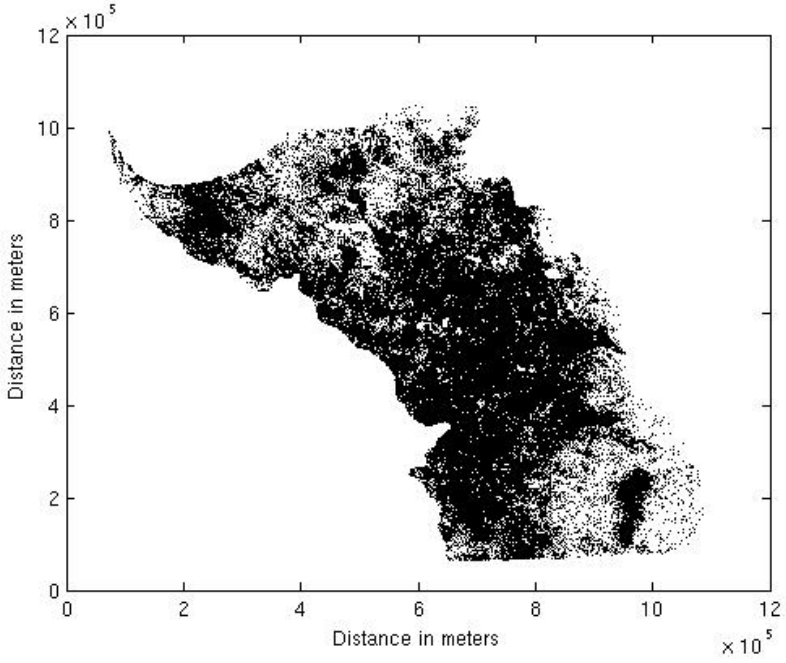

Figure 1.6: The locations of the active and abandoned oil, gas and water wells in the Alberta Basin based on coordinates by the Alberta Geological Survey [6].

Chapter 2

Solution Approaches

In this chapter, solution approaches will be given to the groundwater flow equation derived in chapter 1. Prior to the solution approaches, the motivation behind solving the problem is explained.

2.1 Motivation

In order to do large scale deployment of CO_2, the ability to estimate the large scale flow and leakage of the CO_2 is crucial. Because suitable aquifers for geological storage are often locations for oil and gas reservoirs, there are potentially hundreds of thousands of wells perforating the overlying aquitard. This result in potential pathways for the CO_2 and the brine to leak.

North America has the highest number of oil and gas wells and the highest spatial density in the world, illustrated in figure 2.1. The Alberta Basin presented in section 1.5 is a potential site for large scale deployment of CO_2. However, tools need to be made to be able to estimate the flow and leakage due to the existence of abandoned wells in extensive domains. The first step in order to develop a model that can solve the problem, is by looking at single-phase simplified system.

2.2 ELSA

ELSA is an anonym for Estimating Leakage Semi-Analytically, and is an approach for solving flow problems consisting of abandoned wells. The approach is introduced in [8] by Nordbotten et al., and returns a semi-analytical model for estimating the leakage rates through abandoned wells. Instead of using a grid, the wells are coupled together

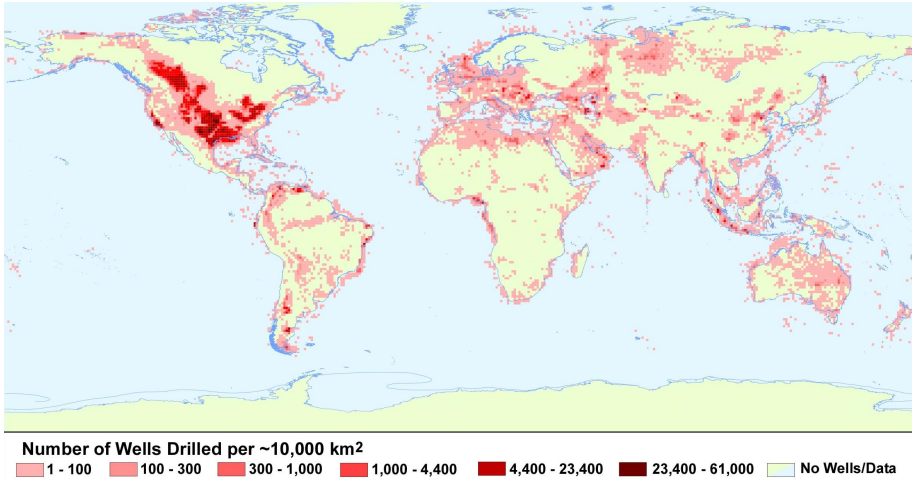

Figure 2.1: Density of wells drilled across the world from the IPCC report in 2005 on Carbon Dioxide Capture and Storage [7].

by the distance between them, illustrated in figure 2.2. The model returns an estimate for the hydraulic head in the wells, which is used in approximating the leakage rates.

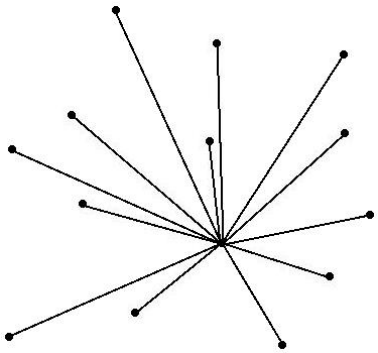

Figure 2.2: An illustration of the relation between one well and the other wells in the ELSA approach.

2.2.1 Well Leakage Model

Recall the governing groundwater flow equation derived in chapter 1

$$S\frac{\partial h}{\partial t} - T\nabla^2 h + \psi_T - \psi_B = Q\delta(\mathbf{x} - \mathbf{x}_w), \tag{2.1}$$

where the Dirac delta function has be introduced in the flux term due to the existence of multiple wells, and the location of a well is denoted $\mathbf{x}_w$. In order to derive a well leakage model from equation (2.1) by the ELSA approach, an aquifer of infinite areal extent is considered. The flow is assumed essentially horizontal and radial to or from the wells. For simplicity, the system consists of two aquifers separated by an aquitard illustrated in figure 2.3. The bottom aquifer is considered as leaky and the hydraulic head in the upper aquifer is assumed constant. Because the bottom aquifer is leaky, there will be water flowing essentially vertical through the aquitard. From [2], the flux of leakage through the aquitard is defined as

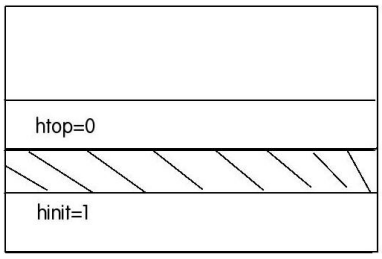

Figure 2.3: An illustration of a system consisting of two aquifers separated by an aquitard, where the hydraulic head in the upper aquifer is equal to zero and the initial hydraulic head in the bottom aquifer is equal to one.

$$\psi_T = -K_{ad}\frac{h_{top} - h}{B}, \tag{2.2}$$

where K_{ad} is the hydraulic conductivity of the aquitard, h_{top} is the hydraulic head in the upper aquifer and B is the thickness of the aquitard. Since there are no leakage downwards, $\psi_B = 0$. In order to estimate the leakage rate on a time aspect of hundreds to thousands of years later after the injection, one can assume the problem is in a equilibrium. First, consider a well problem consisting of one passive well. This implies that the flux in the well can be treated as a boundary condition. In that case, equation (2.1) in radial coordinates on the interval $(0, \infty)$ becomes

$$-T\frac{1}{r}\frac{d}{dr}\left(r\frac{dh}{dr}\right) - K_{ad}\frac{h_{top} - h}{B} = 0, \tag{2.3}$$

where r is denoted as the distance from $\mathbf{x}$ to $\mathbf{x}_w$. For simplicity, assume $h_{top} = 0$ and $h_{init} = 1$. Equation (2.3) may then be expressed as

$$\frac{1}{r}\frac{d}{dr}\left(r\frac{dh}{dr}\right) - \frac{K_{ad}}{TB}h = 0. \tag{2.4}$$

By denoting the radius of the domain as R, boundary conditions can be expressed as

$$\begin{aligned} h(R) &= h_{init} = 1, \\ \lim_{r\to 0} 2\pi r T\frac{\partial h}{\partial r} &= -Q. \end{aligned} \tag{2.5}$$

When writing out the brackets in equation (2.4) and multiplying by r^2, the equation can be expressed as

$$r^2\frac{d^2h}{dr^2} + r\frac{dh}{dr} - r^2\frac{K_{ad}}{BT}h = 0. \tag{2.6}$$

In order to find a solution to equation (2.6), a new term for the radius is introduced as $r' = cr$, where $c = \sqrt{\frac{Kad}{BT}}$. Equation (2.6) may then be formulated as

$$r'^2\frac{d^2h}{dr'^2} + r'\frac{dh}{dr'} - r'^2h = 0. \tag{2.7}$$

Since equation (2.7) is a second-order differential equation, there must be two linearly independent solutions. From Abramowitch and Stegun in [9], equation (2.7) can be recognized as a variant of the modified Bessel equation,

$$x^2\frac{d^2y}{dx^2} + x\frac{dy}{dx} - (x^2+\gamma^2)y = 0. \tag{2.8}$$

The problem (2.8) has two linearly independent solutions, $I_\gamma(x)$ and $K_\gamma(x)$, that are exponentially growing and decaying functions, respectively. $I_\gamma(x)$ is known as a first kind modified Bessel function and $K_\gamma(x)$ as a second kind. Because $\gamma = 0$ in equation (2.7), the solution becomes

$$h(r') = \alpha K_0(r') + \beta I_0(r'), \tag{2.9}$$

where α and β are constants and K_0 and I_0 are of order zero. K_0 goes to infinity towards the well and I_0 goes to infinity towards the boundary. Refer to [9] for more details. The constants α and β are determined by the boundary conditions in equation (2.5). However, equation (2.9) is a solution to a one-well problem. In order to use the solution for problems consisting of more than one well, the problem is divided into two problems with different boundary conditions.

Problem 1: A Boundary Problem

The first problem is a boundary problem, where there exist no wells. The solution can then be stated as

$$h_R(r') = \alpha_R K_0(r') + \beta_R I_0(r'), \tag{2.10}$$

with boundary conditions

$$\begin{aligned} &h_R(r' = cR) = 1, \\ &\lim_{r\to 0}\ 2\pi crT\frac{\partial h_R(r')}{\partial r'} = 0. \end{aligned} \tag{2.11}$$

In order to find the constants in equation (2.10), one can start by using the second boundary condition. The derivative of equation (2.10) becomes

$$\frac{\partial h_R}{\partial r} = c\frac{\partial h_R}{\partial r'} = c[\alpha_R K_1(r') + \beta_R I_1(r')]. \tag{2.12}$$

where $\frac{\partial K_0}{\partial r'} = -K_1$ and $\frac{\partial I_0}{\partial r'} = I_1$ from [9]. Since $I_1(0) = 0$, $\lim_{r\to 0} I_1(r') = 0$. The behavior of the second order modified Bessel function as r reaches zero is found in [9] and states that

$$\lim_{r\to 0} K_1(r') \sim \frac{1}{cr}. \tag{2.13}$$

By equation (2.13), the mass conservation condition in equation (2.11), gives the following relationship

$$\lim_{r\to 0}\ 2\pi crT\alpha_R K_1(r') = \lim_{r\to 0}\ 2\pi crT\alpha_R\frac{1}{cr} = 2\pi T\alpha_R = 0, \tag{2.14}$$

which results in α_R=0. The constant β_R is then given by the outer boundary condition in equation (2.11)

$$h_R(cR) = \beta_R I_0(cR) = 1 \quad \Rightarrow \quad \beta_R = \frac{1}{I_0(cR)}. \tag{2.15}$$

The solution to the first problem is then expressed as

$$h_R(r) = \frac{I_0(cr)}{I_0(cR)}, \tag{2.16}$$

where cr has been substituted for r'.

Problem 2: A Single Well Problem

The second problem is a problem consisting of a well where the hydraulic head is equaled to zero on the boundary, which gives the solution

$$h_w(r') = \alpha_w K_0(r') + \beta_w I_0(r'). \tag{2.17}$$

The boundary conditions are

$$\begin{aligned} &h_w(r' = cR) = 0, \\ &\lim_{r \to 0} \; 2\pi c r T \frac{\partial h_w(r')}{\partial r'} = -Q. \end{aligned} \tag{2.18}$$

By the same procedure as for the first problem, the flux condition in equation (2.18) gives that

$$\alpha_w = \frac{Q}{2\pi T}. \tag{2.19}$$

The outer boundary condition in equation (2.18) gives then the last constant

$$\beta_w = -\frac{Q}{2\pi T} \frac{K_0(cR)}{I_0(cR)}, \tag{2.20}$$

and the solution to the second problem can be expressed as

$$h_w(r) = \frac{Q}{2\pi T} \left[K_0(cr) - \frac{K_0(cR)}{I_0(cR)} I_0(cr) \right], \tag{2.21}$$

where cr has been substituted for r'.

Solution to a Multiple Well Problem

The solution to a problem of one well with $h(cR) = 1$ can be given by a summation of the solution to the first and the second problem

$$h(r) = h_R + h_w = \frac{I_0(cr_o)}{I_0(cR_o)} + Q \frac{1}{2\pi T} \left[K_0(cr) - \frac{K_0(cR)}{I_0(cR)} I_0(cr) \right], \tag{2.22}$$

where r_o is the distance between r and the origin of the domain and R_o is the radius of the domain. In order to get a solution to a problem that contains several wells, superposition can be applied to equation (2.22) due to the linearity in the equation. The solution to a system of N_w wells, may then be expressed as

$$h(r) = \frac{I_0(cr_o)}{I_0(cR_o)} + \sum_{i=1}^{N_w} Q_i \frac{1}{2\pi T}\left[K_0(cr_i) - \frac{K_0(cR_i)}{I_0(cR_i)} I_0(cr_i)\right], \tag{2.23}$$

where r_i is the distance between r and well i and R_i is the distance from r to the boundary. The flux rate through an abandoned well is defined in [8] as

$$Q = K_{well}\pi r_w^2 \frac{h_{top} - h}{B}, \tag{2.24}$$

where K_{well} is the hydraulic conductivity in the well, r_w is the radius of the well and B is the thickness of the aquitard. By inserting the expression (2.24) for the leakage in an abandoned well in equation (2.23), an ELSA well leakage model is achieved

$$\begin{aligned} h(r) = \frac{I_0(cr_o)}{I_0(cR_o)} &+ \sum_{i=1}^{N_{IW}} Q_i \frac{1}{2\pi T}\left[K_0(cr_i) - \frac{K_0(cR_i)}{I_0(cR_i)} I_0(cr_i)\right] \\ &+ \sum_{j=1}^{N_{PW}} K_{well,j}\pi r_{w,j}^2 \frac{h_{top,j} - h_j}{B} \frac{1}{2\pi T}\left[K_0(cr_j) - \frac{K_0(cR_j)}{I_0(cR_j)} I_0(cr_j)\right], \end{aligned} \tag{2.25}$$

where N_{IW} and N_{PW} is the number of injection and abandoned wells, respectively. Equation (2.25) may be solved for the hydraulic head in the passive wells, and from equation (2.24), the estimated hydraulic head returns an estimate for the leakage rate in the abandoned wells. Even though equation (2.25) solves a two-aquifer-one-aquitard system, the solution extends directly to a multi layered system of aquifers. Refer to [8] and [10] for more details.

2.3 The Finite Element Method

The finite element method (FEM) is a numerical method used to solve partial differential equations. The method discretizes the problems by introducing a space consisting of finite elements. By introducing test functions and defining basis functions that span the elements, the bilinear and linear form of the problem is established. Hence, the solution to the problem can be estimated.

2.3.1 Well Leakage Model

Recall the governing equation (1.41)

$$S\frac{\partial h}{\partial t} - T\nabla^2 h + \psi_T - \psi_B = Q\delta(\mathbf{x} - \mathbf{x}_w), \tag{2.26}$$

where the Dirac delta function has be introduced in the flux term due to the existence of multiple wells, and the location of a well is denoted $\mathbf{x}_w$. For simplicity, lets assume the same simplified system as in section 2.2. Equation (2.26) then becomes

$$S\frac{\partial h}{\partial t} - T\nabla^2 h + \frac{K_{ad}}{B}h = Q\delta(\mathbf{x} - \mathbf{x}_w). \tag{2.27}$$

In order to seek a finite element solution to the groundwater flow equation (2.27), the bilinear and the linear form of the equation must be derived [11]. Lets denote the domain by Ω. By choosing triangles as the elements, the domain Ω is triangulated. A reference triangle is introduced, and is illustrated in figure 2.4 together with the triangulation of the domain.

A test function on Ω is denoted by an arbitrary continuous function g, where g' is piecewise continuous and bounded on Ω and $g(\partial\Omega) = 0$. From equation (2.27), the solution must hold for linear functions. Therefore, a finite-dimensional subspace V_l is constructed, where V_l is a set of test functions that are linear on each element $K_l \in \Omega$. Multiplying the problem (2.27) by a test function and integrating over the domain results in

$$\int_\Omega \left[S\frac{\partial h}{\partial t} - T\nabla^2 h + \frac{K_{ad}}{B}h \right] g d\mathbf{x} = \int_\Omega Q\delta(\mathbf{x} - \mathbf{x}_w) g d\mathbf{x}. \tag{2.28}$$

The second term on the left side of equation (2.28) may be expressed by partial integration as

$$\int_\Omega T\nabla^2 h \cdot g d\mathbf{x} = -\int_\Omega T\nabla h \nabla g d\mathbf{x} + Tg\nabla h\Big|_{\partial\Omega} = -\int_\Omega T\nabla h \nabla g d\mathbf{x}, \tag{2.29}$$

because $g(\partial\Omega) = 0$. From equation (2.29), equation (2.28) becomes

$$\int_\Omega \left[S\frac{\partial h}{\partial t} g + T\nabla h \nabla g + \frac{K_{ad}}{B}hg \right] d\mathbf{x} = \int_\Omega Q\delta(\mathbf{x} - \mathbf{x}_w) g d\mathbf{x}. \tag{2.30}$$

The derivative of the hydraulic head with respect to time can be written as

$$\frac{\partial h}{\partial t} = \frac{h^n}{\Delta t} - \frac{h^{n-1}}{\Delta t}, \tag{2.31}$$

where n denotes which time step, Δt is the length of the time interval and h_0 is the initial hydraulic head. When equation (2.31) is applied to equation (2.30), the equation is solved for the time step n. Hence,

$$\int_\Omega \left[S\frac{h^n}{\Delta t}g + T\nabla h^n \nabla g + K_{ad}\frac{h^n}{B}g \right] d\mathbf{x} = \int_\Omega \left[Q\delta(\mathbf{x}-\mathbf{x}_w)g + S\frac{h^{n-1}}{\Delta t}g \right] d\mathbf{x}. \tag{2.32}$$

The integral in equation (2.32) can be partitioned into a summation of the integral of each triangle in the triangulation of Ω. Equation (2.32) for one triangle K_l is then

$$\int_{K_l} \left[S\frac{h_l^n}{\Delta t}g + T\nabla h_l^n \nabla g + K_{ad}\frac{h_l^n}{B}g \right] d\mathbf{x} = \int_{K_l} \left[Q\delta(\mathbf{x}-\mathbf{x}_w)g + S\frac{h_l^{n-1}}{\Delta t}g \right] d\mathbf{x}. \tag{2.33}$$

The integral of the rate through the wells can be expressed as

$$\begin{aligned} \int_{K_l} Q\delta(\mathbf{x}-\mathbf{x}_w)g d\mathbf{x} &= \int_{K_l} Q_{IW}\delta(\mathbf{x}-\mathbf{x}_w)g d\mathbf{x} + \int_{K_l} Q_{PW}\delta(\mathbf{x}-\mathbf{x}_w)g d\mathbf{x} \\ &= \sum_{i=1}^{N_{IW}\in K_l} Q_i g(\mathbf{x}_i) + \sum_{j=1}^{N_{PW}\in K_l} Q_j g(\mathbf{x}_j), \end{aligned} \tag{2.34}$$

where N_{IW} and N_{PW} denotes the number of injection wells and abandoned wells, respectively. By the expression for the rate through an abandoned well (2.24) and the assumption that $h_{top} = 0$, the equation (2.33) becomes

$$\begin{aligned} &\int_{K_l} \left[S\frac{h_l^n}{\Delta t}g + T\nabla h_l^n \nabla g + K_{ad}\frac{h_l^n}{B}g \right] d\mathbf{x} + \sum_{j=1}^{N_{PW}\in K_l} \kappa_j h_l^n g(\mathbf{x}_j) \\ &= \int_{K_l} S\frac{h_l^{n-1}}{\Delta t}g d\mathbf{x} + \sum_{i=1}^{N_{IW}\in K_l} Q_i g(\mathbf{x}_i), \end{aligned} \tag{2.35}$$

where $\kappa = K_{well}\pi r_w^2/B$. The variational problem is then to find a $h_l^n \in V_l$ such that equation (2.35) holds for $\forall g \in V_l$ [11]. From equation (2.35)

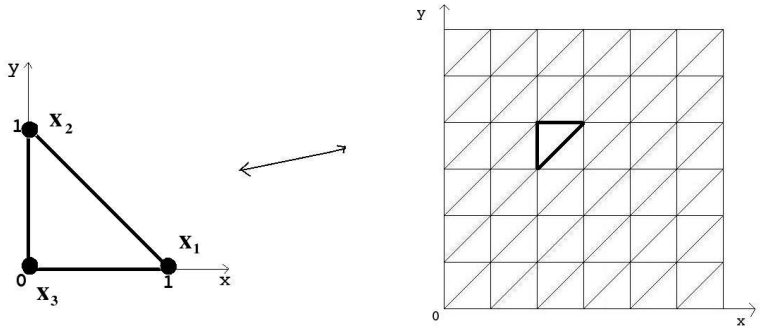

Figure 2.4: An illustration of the triangulation of Ω and the corresponding reference triangle, where the nodes are indicated in the reference triangle.

the bilinear and linear form can be defined as

$$a(h_l^n, g) = \int_{K_l} \left[S\frac{h_l^n}{\Delta t} g + T\nabla h_l^n \nabla g + K_{ad}\frac{h_l^n}{B} g \right] d\mathbf{x} + \sum_{j=1}^{N_{PW}\in K_l} \kappa_j h_l^n g(\mathbf{x}_j), \tag{2.36}$$

$$b(g) = \int_{K_l} S\frac{h_l^{n-1}}{\Delta t} g d\mathbf{x} + \sum_{i=1}^{N_{IW}\in K_l} Q_i g(\mathbf{x}_i), \tag{2.37}$$

for $h_l^n, g \in V_l$. The weak formulation is then: Find a $h_l^n \in V_l$ such that $\forall\ g \in V_l$

$$a(h_l^n, g) = b(g). \tag{2.38}$$

The elements in Ω are chosen to have three nodes, one situated in each corner, see the reference triangle in figure 2.4. Basis functions for V_l are then linear functions that takes the value 1 at the node x_j and the value 0 at the other two nodes in the triangle. For the reference triangle, the three basis functions are chosen as

$$\begin{aligned} \phi_1(x, y) &= x \\ \phi_2(x, y) &= y \\ \phi_3(x, y) &= 1 - x - y. \end{aligned} \tag{2.39}$$

When the values of the test functions in the nodes x_k, $k = 1, 2, 3$, are defined by the parameter $\eta_k = g(x_k)$, the test functions for the reference triangle may be formulated as

$$g(x) = \sum_{k=1}^{3} \eta_k \phi_k(x) \qquad x \in \Omega. \tag{2.40}$$

Substituting the test functions by the basis functions in equation (2.38), the bilinear and linear form can be written as

$$a(h_l^n, \phi_k) = b(\phi_k). \tag{2.41}$$

If equation (2.41) holds, linear combinations of h_l satisfies the variational problem (2.35) [11]. By denoting the estimated hydraulic head in the nodes by $\xi_k = h_l(x_k)$, an expression for the hydraulic head in K_l becomes

$$h_l(x) = \sum_{k=1}^{3} \xi_k \phi_k(x) \qquad x \in \Omega. \tag{2.42}$$

When using equation (2.40) and (2.42) in the bilinear and linear form in equation (2.36) and (2.37), the system of equations for one triangle becomes

$$\begin{aligned} \sum_{k=1}^{3}\sum_{m=1}^{3} a(\phi_k, \phi_m)\xi_k = \int_{K_l} \left[S\frac{\phi_k}{\Delta t}\phi_m + T\nabla\phi_k\nabla\phi_m + K_{ad}\frac{\phi_k}{B}\phi_m \right] d\mathbf{x} \\ + \sum_{j=1}^{N_{PW}\epsilon K_l} \kappa_j \phi_k \phi_m(\mathbf{x}_j), \end{aligned} \tag{2.43}$$

$$\sum_{m=1}^{3} b(\phi_m) = \int_{K_l} \left[Q\delta(\mathbf{x}-\mathbf{x}_w)\phi_m + S\frac{h_l^{n-1}}{\Delta t}\phi_m \right] d\mathbf{x} + \sum_{i=1}^{N_{IW}\epsilon K_l} Q_i \phi_j(\mathbf{x}_i). \tag{2.44}$$

The integrals of the basis functions in equation (2.43) for the reference triangle becomes

$$\int_0^1 \int_0^{1-x} \phi_k \phi_m d\mathbf{x} = \begin{cases} 1/12 & k=m \\ 1/24 & k \neq m \end{cases} \tag{2.45}$$

and

$$\int_0^1 \int_0^{1-x} \nabla\phi_k \nabla\phi_m d\mathbf{x} = \begin{bmatrix} 1/2 & 0 & -1/2 \\ 0 & 1/2 & -1/2 \\ -1/2 & -1/2 & 1 \end{bmatrix} \; for \; k, m = 1, 2, 3. \tag{2.46}$$

In equation (2.44), the integral of the basis functions returns

$$\int_0^1 \int_0^{1-x} \phi_m d\mathbf{x} = 1/6. \tag{2.47}$$

Since the triangles have corresponding nodes to other triangles, illustrated in figure 2.5, a matrix for the nodes can be made and

$$A\xi = b, \tag{2.48}$$

where A is the matrix of all the nodes in the triangulation and ξ and b are vectors. By solving (2.48) for ξ, an estimate for the hydraulic head in each node is achieved.

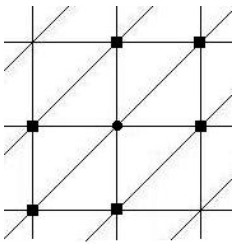

Figure 2.5: An illustration of the relationship in the nodes between the triangles, where one node (circle) may be connected to the maximum of six nodes from different triangles (squares).

Chapter 3

Multiscale Approach

In this chapter, a multiscale approach is derived in order to try to solve the groundwater flow problem when there is hundreds of thousand of abandoned wells. However, in the determination of the size of the fine scale domains, it is clear that the well leakage problem is not a multiscale problem. This is shown in section 3.4, and in section 3.5 implications of the multiscale model are introduced and discussed.

3.1 Motivation

Extensive domains may contain hundreds of thousand of abandoned wells where one example is the Alberta basin presented in chapter 1. When the leakage rates through the aquitard decreases the number of wells a well will affect increases. An attempt to solve problems of this kind is by introducing a multiscale model for the system. The idea is that the model would estimate the large scale flow and leakage and use already derived well leakage models for the fine scale and the coarse scale.

3.2 Multiscale Methods

Multiscale methods couples different models with levels of detail in order to achieve a balance between accuracy and efficiency [12]. One method is called the Heterogeneous Multiscale Method where the macroscale process and problem is of interest. The macroscale solution can be denoted by U. Since the macroscale model is not valid everywhere, one can use the knowledge from the microscopic process. The solution on the microscopic scale can be denoted by u. The two processes are related to each

other by a compression and a reconstruction operator. When a compression and a reconstruction operator are denoted as Q and R, respectively, the scales are related by $Qu = U$ and $RU = u$ where $QR = I$ when I is the identity operator.

3.3 Multiscale Well Leakage Model

Since the HMFEM framework provides an implicit description of the coarse flux expression based on the fine scale model [2], the approach taken in this context will be based on the HMFEM way of thinking.

3.3.1 Coarse Scale Solver

For the groundwater flow problem, the coarse scale is chosen as a triangulation of the domain. The FEM is then an appropriate coarse scale solver and was derived in chapter 2. However, the derived finite element well leakage model solves a problem on a fine scale. The difference on the coarse scale is that the leakage rate through the abandoned wells are estimated on the fine scale. An average of these estimates scales the leakage rate on the coarse scale, which is the compression for the groundwater flow problem. The reconstruction is then to solve the problem on a smaller domain by the fine scale solver. To relate the coarse scale equation to the fine scale, lets consider the groundwater flow problem on the coarse scale

$$S\frac{\partial h}{\partial t} - T\nabla^2 h + \frac{K_{ad}}{B}h = Q\delta(\mathbf{x} - \mathbf{x}_w). \tag{3.1}$$

The same approach as in chapter 2 for the FEM gives the problem

$$\begin{aligned} &\int_{K_l}\left[S\frac{h_l^n}{\Delta t}g + T\nabla h_l^n \nabla g + K_{ad}\frac{h_l^n}{B}g\right]d\mathbf{x} \\ &= \sum_{i=1}^{N_{IW}\epsilon K_l} Q_{IW}(\mathbf{x}_i)g + \int_{K_l}\left[Q_{PW}\delta(\mathbf{x} - \mathbf{x}_w) + S\frac{h_l^{n-1}}{\Delta t}\right]g d\mathbf{x} \end{aligned} \tag{3.2}$$

The integral of the flux rate through the abandoned wells can be expressed by using a Gaussian quadrature rule. A Gaussian quadrature rule is an approximation to a definite integral of a function, where the integral is expressed as a summation of the function evaluated in the

quadrature points multiplied by a corresponding weight [13]. The integral of the abandoned wells in equation (3.2) by the use of a Gaussian quadrature rule may then be written as

$$\int_{K_l} Q_{PW}(\mathbf{x})\delta(\mathbf{x}-\mathbf{x}_w)gd\mathbf{x} \approx |K_l| \sum_{p=1}^{N_{GQ}} \omega_p Q_{PW}(\mathbf{x}_p)g(\mathbf{x}_p)\delta(\mathbf{x}_p-\mathbf{x}_w), \quad (3.3)$$

where N_{GQ} is the number of quadrature points and ω_p is the weight corresponding to point p. Since the elements are large with many abandoned wells, the evaluation points may be seen as a ball B with a center in the point and a radius ε. Equation (3.3) may then be written as

$$\int_{K_l} Q_{PW}(\mathbf{x})\delta(\mathbf{x}-\mathbf{x}_w)gd\mathbf{x} \approx |K_l| \sum_{p=1}^{N_{GQ}} \omega_p \frac{\int_{B_p} Q_{PW} g d\mathbf{x}}{\pi\varepsilon_p^2}. \quad (3.4)$$

Figure 3.1 illustrates the quadrature points inside a triangle. Because the ball is very small compared to the size of the triangle, the variation of the test function g are not significant and may therefore be placed outside of the integral. The leakage rate in the quadrature points is an average of the fine scale leakage rate in B_p, and scales the difference on the coarse scale between the hydraulic head in the aquifer and the aquifer above. Equation (3.4) may then be expressed as

$$\int_{K_l} Q_{PW}(\mathbf{x})\delta(\mathbf{x}-\mathbf{x}_w)gd\mathbf{x} \approx |K_l| \sum_{p=1}^{N_{GQ}} \omega_p G^p(h_{top} - h_l^n(\mathbf{x}_p))g(\mathbf{x}_p), \quad (3.5)$$

where G^p is the compression of the fine scale

$$G^p = \frac{1}{\pi\varepsilon^2} \frac{\sum_{j=1}^{N_w \in B_p} Q_j}{h_{top} - h_{init}}. \quad (3.6)$$

The number of wells in B_p in equation (3.5) is denoted N_w. Equation (3.5) substituted in equation (3.2) gives the coarse scale bilinear and linear terms

$$a(h_l^n, g) = \int_{K_l} \left[S\frac{h_l^n}{\Delta t}g + T\nabla h_l^n \nabla g + K_{ad}\frac{h_l^n}{B}g \right] d\mathbf{x} + |K_l| \sum_{p=1}^{N_{GQ}} \omega_p G^p h_l^n(\mathbf{x}_p)g(\mathbf{x}_p), \quad (3.7)$$

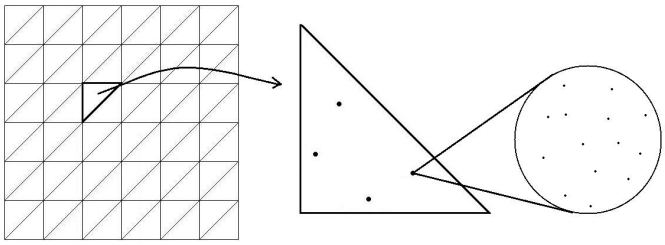

Figure 3.1: An illustration of the quadrature points inside a triangle in the triangulation of the domain. These points are given a radius, and there might be several wells inside the circle that is made up by the quadrature point and the radius.

$$b(g) = \sum_{i=1}^{N_{IW} \in K_l} Q_{IW}(\mathbf{x}_i)g + |K_l| \sum_{p=1}^{N_{GQ}} \omega_p G^p h_{top}(\mathbf{x}_p) g(\mathbf{x}_p) + \int_{K_l} S \frac{h_l^{n-1}}{\Delta t} g d\mathbf{x}, \tag{3.8}$$

for $h_l^n, g \in V_l$. The coarse scale solution may now be estimated from equation (3.7) and (3.8) by the same procedure as in section 2.3.

3.3.2 Fine Scale Solver

On the fine scale, the well leakage model derived by the ELSA approach is chosen to determine the leakage rate. The problem was assumed steady-state in section 2.2, which is a good assumption because the domain reaches equilibrium much faster on a smaller area than on the coarse scale. From chapter 2, an estimate of the hydraulic head on the fine scale is obtained by solving the system of equations

$$h(r) = \frac{I_0(cr_o)}{I_0(cR_o)} + \sum_{i=1}^{N_{PW}} K_{well,i} \pi r_{w,i}^2 \frac{h_{top,i} - h_i}{2\pi TB} \left[K_0(cr_i) - \frac{K_0(cR_i)}{I_0(cR_i)} I_0(cr_i) \right], \tag{3.9}$$

where the injection wells are placed outside the quadrature circles and

$$c = \sqrt{\frac{K_{ad}}{BT}}. \tag{3.10}$$

The hydraulic heads are then used in determine the leakage rate in the abandoned wells by

$$Q_i = K_{well,i} \pi r_{w,i}^2 \frac{h_{top,i} - h_i}{B}. \tag{3.11}$$

3.4 Scale Issues

In the previous section a multiscale approach was applied to the well leakage models derived in chapter 2 in order to achieve a multiscale model. Quadrature points was introduced, and a radius for these still needs to be decided. In this section, an expression for the relative error for the analytical solution and an approximated solution on a ball for the fine scale groundwater problem is derived. The ball can be considered as a quadrature point with a radius and the relative error is used in the discussion of a suitable radius for the quadrature points.

Lets start the derivation by considering the fine scale problem

$$-T\nabla^2 h + \frac{K_{ad}}{B}h = Q\delta(\mathbf{x} - \mathbf{x}_w), \tag{3.12}$$

where the domain is assumed to be infinite. The Greens function to equation (3.12) is the fundamental solution in the ELSA approach and is expressed as

$$G_c^{R^2}(\mathbf{x}, \mathbf{x}_w) = \frac{1}{2\pi T} K_0(c|\mathbf{x} - \mathbf{x}_w|) \tag{3.13}$$

since the the domain is infinite. Refer to [14] for more details. The solution to equation (3.12) may be written in terms of equation (3.13) as

$$h(\mathbf{x}) = Q * G_c^{R^2} = \int_{R^2} G_c^{R^2}(\mathbf{x}, \mathbf{x}_w) Q(\mathbf{x}_w) d\mathbf{x}_w. \tag{3.14}$$

In order to make an approximation to the solution equation (3.14), a ball of radius δ is considered. By transforming the origin to the center of the ball $\mathbf{x}_w \to \mathbf{x} + \mathbf{x}_w$, the solution on the ball becomes

$$\begin{aligned} h^\delta(\mathbf{x}) &= \int_{B(\mathbf{x};\delta)} G_c^{R^2}(\mathbf{x}, \mathbf{x} + \mathbf{x}_w) Q(\mathbf{x} + \mathbf{x}_w) d\mathbf{x}_w \\ &= \int_{R^2} H(\delta - |\mathbf{x} - \mathbf{x}_w|) G_c^{R^2}(\mathbf{x}, \mathbf{x}_w) Q(\mathbf{x}_w) d\mathbf{x}_w \\ &= \int_{R^2} G_c^{\delta}(\mathbf{x}, \mathbf{x}_w) Q(\mathbf{x}_w) d\mathbf{x}_w, \end{aligned} \tag{3.15}$$

where $B(\mathbf{x}; \delta)$ is a ball centered in $\mathbf{x}$ with a radius δ and H is the Heaviside step function. The error between the solution on the ball and the solution on the entire domain can be obtained by considering the integral of the difference between equation (3.14) and equation (3.15), expressed as

$$\begin{aligned}\int_{R^2} h - h^\delta d\mathbf{x} &= \int_{R^2}\int_{R^2} [G_c^{R^2} - G_c^\delta](\mathbf{x}, \mathbf{x}_w) Q(\mathbf{x}_w) d\mathbf{x}_w d\mathbf{x} \\ &= \int_{R^2}\int_{R^2} [G_c^{R^2} - G_c^\delta](\mathbf{x}, \mathbf{x}_w) d\mathbf{x} Q(\mathbf{x}_w) d\mathbf{x}_w.\end{aligned} \tag{3.16}$$

The absolute value of equation (3.16) becomes

$$|\int_{R^2} h - h^\delta d\mathbf{x}| = |\int_{R^2}\int_{R^2} [G_c^{R^2} - G_c^\delta](\mathbf{x}, \mathbf{x}_w) d\mathbf{x} Q(\mathbf{x}_w) d\mathbf{x}_w|, \tag{3.17}$$

Equation (3.17) can be written in terms of the ℓ_1 norm. By using Cauchy-Schwartz inequality the relationship becomes

$$\| h - h^\delta \| \leq \| \int_{R^2} [G_c - G_c^\delta] d\mathbf{x} \| \| Q \| . \tag{3.18}$$

When the differential operator in equation (3.12) is denoted L, following relationship is valid

$$\| Q \| = \| Lh \| \leq \| L \| \| h \| . \tag{3.19}$$

By equation (3.19), equation (3.18) may be written as

$$\| h - h^\delta \| \leq \| \int_{R^2} [G_c - G_c^\delta] d\mathbf{x} \| \| L \| \| h \| . \tag{3.20}$$

Thus,

$$\frac{\| h - h^\delta \|}{\| h \|} \leq \| \int_{R^2} [G_c - G_c^\delta] d\mathbf{x} \| \| L \| . \tag{3.21}$$

The relationship between the Green function and the differential operator $\| L \| \sim 1/ \| \int_{R^2} G_c d\mathbf{x} \|$, may be used to rewrite equation (3.21) as

$$\frac{\| h - h^\delta \|}{\| h \|} \leq \frac{\| \int_{R^2} [G_c - G_c^\delta] d\mathbf{x} \|}{\| \int_{R^2} G_c d\mathbf{x} \|}. \tag{3.22}$$

Equation (3.22) expresses the relative error in the hydraulic head estimated on a ball of radius δ. The ball may be considered as the circle around a quadrature point. From [2], a leaky well in an aquifer draws 95% of its water from leakage within a radial distance of $4/c$, and 99% of its water in a radius $5/c$. This distance is referred to as the radius of influence and is a natural choice as the radius of the circles around the

quadrature points. By equation (3.22), the hydraulic head on the coarse scale only affects the fine scale by one percent if $\delta = 5/c$. This indicates that the multiscale approach in section 3.3 returns a model that is not a multiscale model. Therefore, the model in section 3.3 is not able to estimate large scale flow and leakage.

3.5 Implication for Multiscale Models of Leaky Aquifers

From section 3.4, the well leakage model composed by the FEM and the ELSA approach will not be a multiscale system. The model is therefore not able to return physical realistic estimates for the large scale flow and leakage. However, there might be modifications that can be made in the coupling of the methods that might give a multiscale structure. Thus, three examples for different modification approaches to the coupling of the models in section 3.3 are introduced.

The first approach is to use the well leakage model derived from the ELSA approach to estimate the behavior on entire elements. This is done instead of using a Gaussian quadrature rule because the scale problem occurred in the determination of the size of the circles around the quadrature points. However, more complicated grid conditions are required and it is computational demanding to solve entire grid blocks by the ELSA approach due to the high amount of wells located in an element.

A second example is to couple the time scales on the fine scale and the coarse scale together in a different way. In the derivation of the model in section 3.3, the fine scale is assumed to be in equilibrium. This might not be a good assumption since both the FEM and the ELSA model is then on the same time scale. By introducing local time steps on the fine scale one could estimate the changes between these steps and upscale the change to the coarse scale. This might return a multiscale structured system.

The flux through an aquitard is defined in chapter 1 as the hydraulic head times the ratio between the hydraulic conductivity of the aquitard and its thickness. However, the flux in an aquitard is small compared to the flux in an abandoned well. One could imagine that a compression of the aquitard occurs. As a last example of changes to the derived well leakage model in section 3.3, one may include more physics on the fine scale such as a compression of the aquitard. This might return a multiscale structure when combined by a coarse scale solver.

Chapter 4

Illustrative Examples

In this chapter, the FEM and the ELSA well leakage model are compared for three examples followed by and example that illustrates the characteristics of the coupled well leakage model.

4.1 Verification of the Models by the FEM and the ELSA approach

To verify the well leakage models derived by the FEM and the ELSA approach in chapter 2, three examples are given. All examples have a 4×4 km^2 domain and parameters for the examples are based on [8] and listed in table 4.1.

Parameter	Value	Unit
S	$5 \cdot 10^{-7}$	
K_{aq}	$2 \cdot 10^{-7}$	m/s
K_{ad}	$1 \cdot 10^{-12}$	m/s
K_{well}	$2 \cdot 10^{-4}$	m/s
D	20	m
B	15	m
r_w	0.15	m
h_{top}	0	m
h_{init}	1	m
t_0	0	s
t_1	100	y

Table 4.1: The parameters used in the examples. Based on examples in [8].

4.1.1 Example 1: No Wells

In the first example there are no wells in the domain. Hence, the leakage only occurs through the aquitard. The solution by the ELSA approach when there are no wells is given by the boundary problem solution equation (2.16) in section 2.2.1

$$h(r) = \frac{I_0(cr)}{I_0(cR)}, \tag{4.1}$$

where R=2000. In the derivation of the well leakage models, the boundary and the initial condition of the hydraulic head was equaled to one and the hydraulic head in the upper aquifer was equaled to zero. From Darcy's law (1.7), fluids flow in the direction where the hydraulic head decreases. This implies that water in the aquifer will leak through the aquitard towards the upper aquifer. Because the boundary condition equals the initial condition, the hydraulic head is at its lowest in the center of the domain and increases towards the boundary. This can be seen in figure 4.1, which is the results from the model based on the FEM when there are no wells in the domain and the length of an element is 125 m. In figure 4.2, the FEM solution is compared to the ELSA approach for the cross section of the domain and one can see that the models return similar estimates.

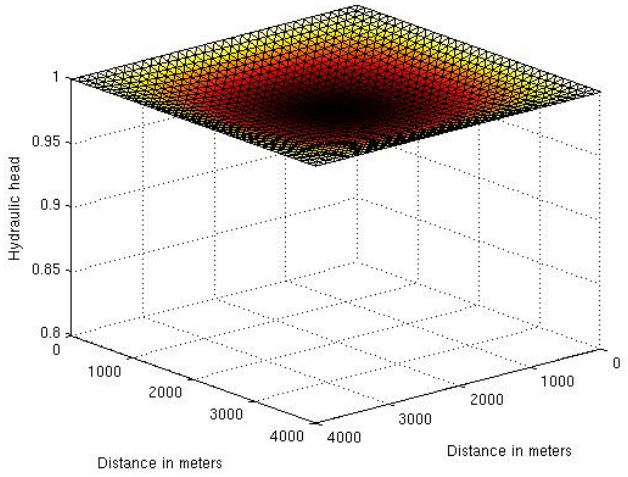

Figure 4.1: Example 1: The hydraulic head estimated by the FEM when there are no wells in the domain and the length of an element is 125 m.

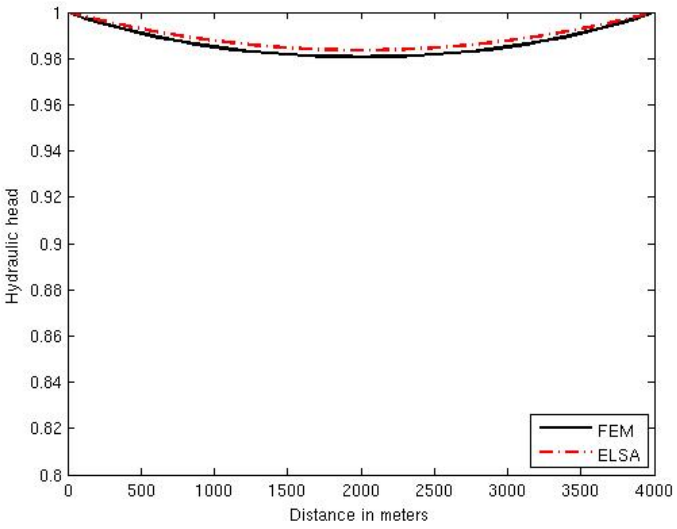

Figure 4.2: Example 1: The hydraulic head estimated by the FEM and the ELSA approach for a cross section of the domain without any wells. The length of an element is 125 m.

4.1.2 Example 2: One Well

In the second example, an abandoned well is situated in the center of the domain. It is then naturally to expect the estimated hydraulic head to be lower than for the example in section 4.1.1, because there is leakage through both the aquitard and the abandoned well. The basis functions in the FEM was chosen as linear functions in chapter 2. In order for the basis function to capture the behavior of the hydraulic head near the well, there has to be enough elements nearby a well. As in example one the length of an element is set to be 125 m. The method is then able to capture an exponential behavior as seen in figure 4.3. For the ELSA model, the Bessel function K_0 is the reason for the exponential behavior towards the well. This can be seen in the figure 4.4, which is the results from the FEM and the ELSA approach for the cross section of the domain. It can also be noticed in figure 4.4 that there is not much difference between the estimates from the different models.

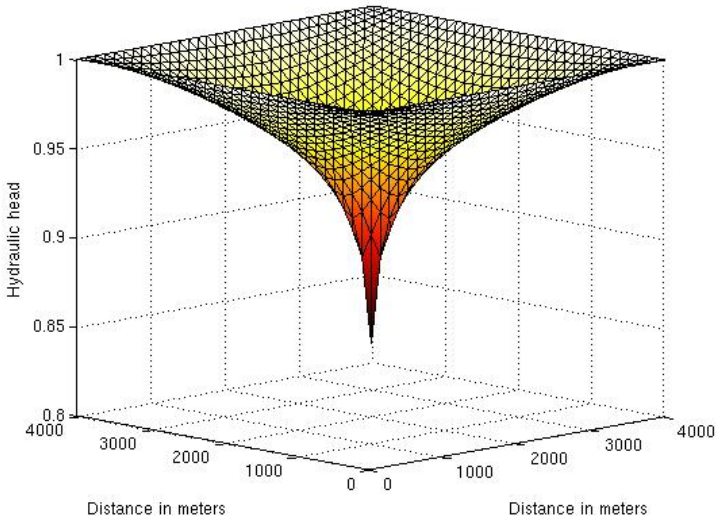

Figure 4.3: Example 2: The hydraulic head estimated by the FEM for the domain when there is one well located in the center of the domain.

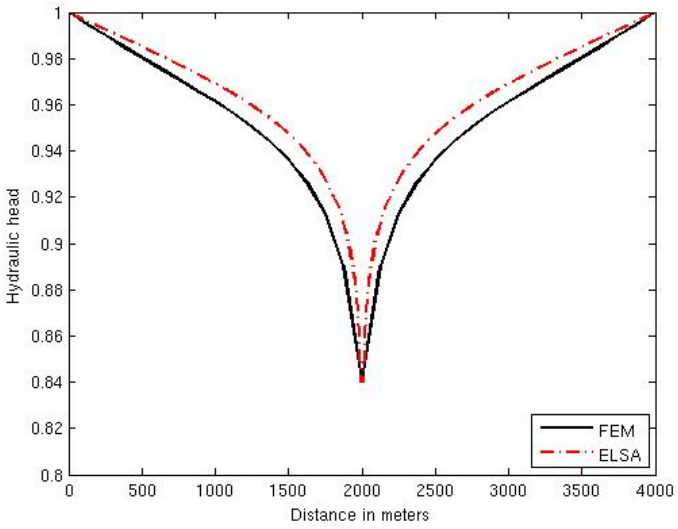

Figure 4.4: Example 2: The hydraulic head estiamted by the FEM and the ELSA well leakage model for a cross section of the domain when one well is located in the center of the domain.

4.1.3 Example 3: Three Wells

In the third example, there are three wells located on the cross section of the domain in a distance of 1000 m from each other. The boundary value is chosen as $h = 0.992$ in the model by the FEM in order to solve the same problem as the model by the ELSA approach does when there are three wells. To find out if the wells affect each others leakage, one may calculate the radius of influence. From section 3.4, a leaky well in an aquifer draws 99% of its water in a radius $5/c$. The radius of influence for each of the three wells is then $5/c = 5/(1.2910 \cdot 10^{-4})$ m ≈ 40 km. Since the distance between the wells are 1000 m, they will affect each others leakage. This can be seen in figure 4.5 and 4.6, where the leakage through the well in the center of the domain is the largest. That is because the well has two neighbors in a 1000 m distance, while the others have one in a 1000 m distance and one in a 2000 m distance. One may also notice that the leakage in the wells in figure 4.6 is larger in comparison with the solution for the problem when there is only one well, figure 4.4.

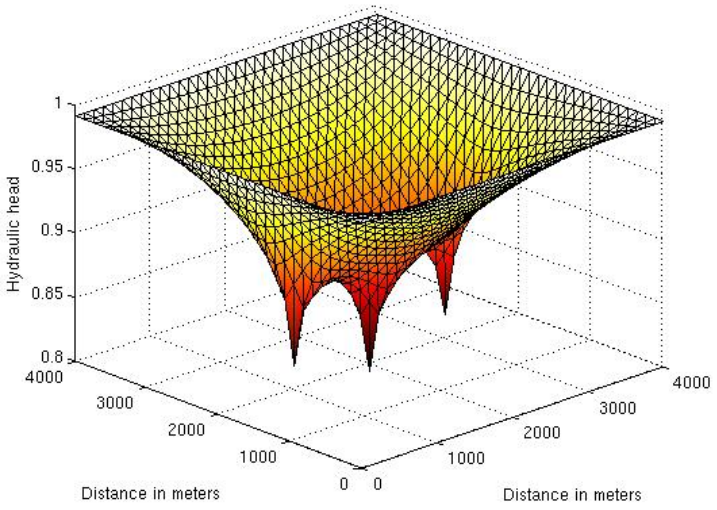

Figure 4.5: Example 3: The hydraulic head estimated by the FEM for the domain when there are three wells located in the domain. These wells are located on the cross section of the domain in a distance of 1000 m from each other.

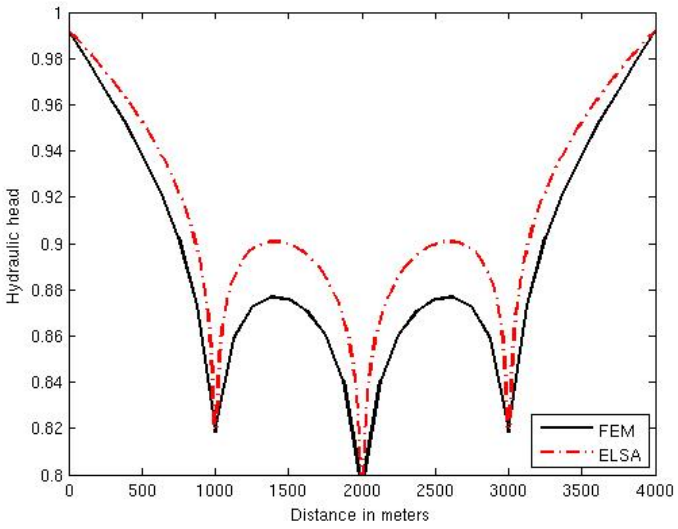

Figure 4.6: Example 3: The hydraulic head estimated by the FEM and the ELSA approach for a cross section of the domain when there are three wells located in the domain. These wells are located on the cross section of the domain in a distance of 1000 m from each other.

4.2 Characteristics of the Coupled Well Leakage Model

In this section, the coupled well leakage model is applied to a problem with an extensive domain. The radius of the quadrature circles are chosen as the radius of influence and the domain is 1600×1600 km^2, which is as extensive as the Alberta Basin introduced in section 1.5. The physics of the domain is based on the parameters listed in table 4.1. For the elements in the FEM, a four point Gaussian quadrature rule is chosen. This implies that the solution is exactly up to a second order. The coordinates for the quadrature points in the reference triangle are illustrated in figure 4.7.

The 99% radius of influence for a well is $5/c \approx 40$ km, and the length of an element in the FEM is then chosen as 400 km, which is ten times the radius of influence. For simplicity, one well is located in each quadrature point. The results when there are more wells located inside the circle around a quadrature point is about the same. The estimate of the hydraulic head by the coupled model is seen in figure 4.8 and in figure

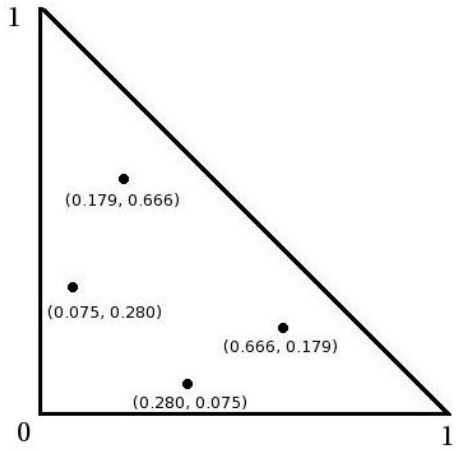

Figure 4.7: An illustration of the location of four quadrature points in the reference triangle when a four point Gaussian quadrature rule is chosen.

4.9 where the solution for the cross section of the domain is illustrated. One may notice that the solution turns negative in some nodes. This is an effect caused by the characteristics of the numerical scheme. If the elements becomes to large outside of the main diagonal, oscillations might occur. For the well leakage problem, it is caused by the discretization of the leakage terms.

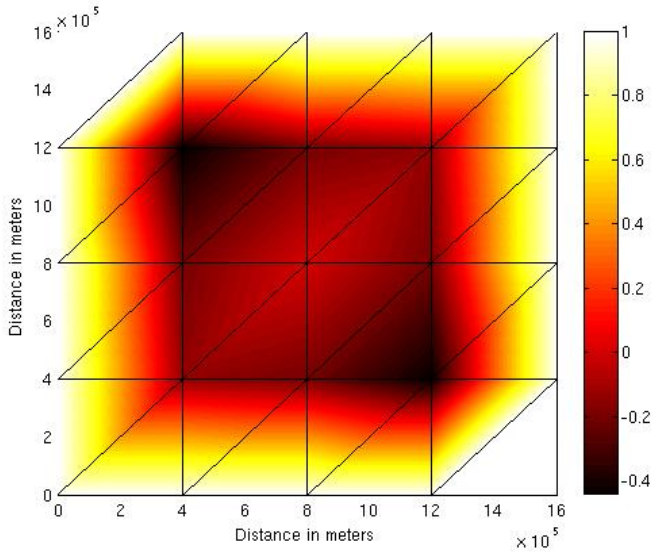

Figure 4.8: The hydraulic head estimated by the coupling of the FEM and the ELSA approach. A four point Gaussian quadrature rule is used and the radius around these points are the radius of influence for a well. In each quadrature point there is one well and the size of an element is 400 km.

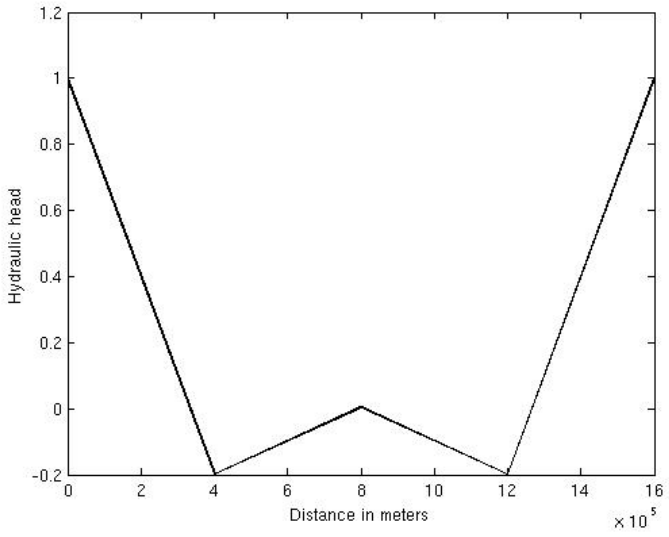

Figure 4.9: The hydraulic head estimated by the coupling of the FEM and the ELSA approach for the cross section of the domain. A four point Gaussian quadrature rule is used and the radius around these points are the radius of influence for a well. In each quadrature point there is one well and the size of an element is 400 km.

Chapter 5

Conclusion

Because of the challenge in estimating the flow and leakage for problems on extensive domains that may contain hundreds of thousands abandoned wells, a well leakage model has been derived by a multiscale approach in order to estimate large scale flow and leakage. The model consist of a coarse and a fine scale solver, which are chosen as a FEM and a ELSA approach to the governing flow equation derived in chapter 1. Since it is the large scale flow and leakage that is of interest, the coarse and the fine scale solver are connected through a compression, section3.3. The compression is an average of the fine scale solution for certain domains on the fine scale. These domains are chosen by a Gaussian quadrature rule applied to each of the elements on the coarse scale. Since the elements are considered as large and therefore contain several wells, the quadrature points are given a radius. The radius indicates the domain where the fine scale solver is used. A natural choice of the radius is the radius of influence for a well [2]. However, as section 3.4 explains the radius of influence implies that a well is hardly affected by the coarse scale. Hence, the coupling of the FEM and the ELSA model do not return a multiscale system.

It is not obvious that a coupling of a coarse and a fine scale solver would not return a multiscale model. However, as the multiscale approach in chapter 3 fails in giving a multiscale structured model, the importance of scale separation is emphasized. In order to have a multiscale system, the coarse and the fine scale problem must have some differences in the physics in the problem they are solving. In this thesis, the idea was that an upscaling of the fine scale averaged leakage rate and use it as a scalar in the leakage term on the coarse scale would return a multiscale system. This turned out to be a wrong approach since a well has a radius of influence, and it illustrates the challenge in estimating

flow on extensive domains with hundreds of thousands abandoned wells like the Alberta Basin introduced in chapter 1.

In section 3.5, modifications to the coupled model derived in chapter 3 was discussed in order to achieve a possible multiscale structure. One example would be to use the ELSA model as a solver on the complete grid block instead of introducing quadrature points while another is to introduce local time steps on the fine scale. The changes in the hydraulic head in the time steps would then be up scaled to the coarse scale. As the last example, more physics could be included on the fine scale such as a compression of the aquitard.

Bibliography

[1] S. E. Gasda, S. Bachu, and M. A. Celia. Spatial characterization of the location of potentially leaky wells penetrating a deep saline aquifer in a mature sedimentary basin. *Environmental geology*, 46(6):707–720, 2004.

[2] J. M. Nordbotten and M. A. Celia. *Geological Storage of CO_2: Modelling Approaches for Large-Scale Simulation*. For publication, Wiley InterScience, 2010.

[3] G. F. Pinder and M. A. Celia. *Subsurface hydrology*. John Wiley and Sons, 2006.

[4] Ø. Pettersen. Lecture Notes. *Department of Mathematics, University of Bergen*, 1990.

[5] R. A. Freeze and J. A. Cherry. *Groundwater*. Prentice Hall, 1979.

[6] Alberta Geological Survey. *Personal Communication*. http://www.ags.gov.ab.ca.

[7] Intergovernmental Panel on Climate Change (IPCC). *Special Report on Carbon Dioxide Capture and Storage*. Cambridge University Press, 2005.

[8] J. M. Nordbotten, M. A. Celia, and S. Bachu. Analytical solutions for leakage rates through abandoned wells. *Water Resources Research*, 40(4):W04204, 2004.

[9] M. Abramowitz and I. A. Stegun. *Handbook of mathematical functions with formulas, graphs, and mathematical tables*. Dover publications, 1964.

[10] B. Hunt. Flow to a well in a multiaquifer system. *Water Resources Research*, 21:1637–1641, 1985.

[11] C. Johnson. *Numerical solution of partial differential equations by the finite element method.* Cambridge University Press, 1987.

[12] W. E, B. Engquist, and Z. Huang. Heterogeneous multiscale method: a general methodology for multiscale modeling. *Physical Review B*, 67(9):092101, 2003.

[13] D. Kincaid and W. Cheney. *Numerical analysis: mathematics of scientific computing.* Brooks/Cole, 2002.

[14] L. Evans. *Partial Differential Equations.* American Mathematical Society, 2000.